

Quasiparticle band structures and interface physics of SnS and GeS

Brad D. Malone¹ and Efthimios Kaxiras^{1,2}

¹*School of Engineering and Applied Sciences, Harvard University, Cambridge, Massachusetts 02138, USA*

²*Department of Physics, Harvard University, Cambridge, Massachusetts 02138, USA*

(Received 9 February 2013; revised manuscript received 15 May 2013; published 24 June 2013)

We perform first-principles, density-functional-theory calculations of the electronic structure for the layered bulk materials SnS and GeS which are of interest for photovoltaic applications. Band gap corrections are computed within the *GW* approximation to the electron self-energy. The resulting quasiparticle gaps in both SnS and GeS are in excellent agreement with the majority of existing experimental measurements. In order to better understand the possible use of GeS layers as a carrier-confining barrier within a SnS-based photovoltaic device, we compute the band offsets for different orientations of a SnS/GeS heterojunction. We find the valence band offsets to be almost independent of interfacial direction while the conduction band offsets show a strong anisotropy as a result of the variation in the band gap caused by epitaxial strain along the different directions.

DOI: [10.1103/PhysRevB.87.245312](https://doi.org/10.1103/PhysRevB.87.245312)

PACS number(s): 71.20.Nr, 73.20.-r

I. INTRODUCTION

Photovoltaics are expected to be an important part of meeting humanity's energy needs, but to fulfill this expectation efficient photovoltaic devices will have to be produced from earth-abundant materials at a reasonable cost.¹ These materials should also be nontoxic to avoid adverse environmental effects. It is partially for these reasons that SnS has attracted recent interest as the absorber material in a photovoltaic device.²⁻⁷ In addition to being made of abundant and nontoxic elements, SnS has a high absorption coefficient near the optical absorption edge of ~ 1.3 eV.^{2,8} Steady progress has been reported toward achieving higher photovoltaic efficiencies in SnS-based cells, from initial maximal values of 1.3%,² to 1.95% using SnS nanowire arrays,⁶ and up to 2.46% using a Zn(O,S) buffer layer.⁷

Despite these advances, the efficiency of SnS cells remains far below the theoretical limit of 24%.³ Greater efficiency might still be achieved in a number of ways: increasing the quality of the SnS samples themselves by reducing defects and/or impurities present in the sample,^{3,7,9} optimizing the device geometry, preventing reflective losses, or obtaining better band alignment with neighboring layers.⁷ GeS, a structure isomorphous to SnS, might be of interest as part of an electron-blocking layer in a solar device utilizing SnS as the absorber layer.¹⁰ The conduction states near the band edge of SnS predominately originate from Sn, while the valence band manifold is shared between the two constituent atoms and is strongly dominated by S states beyond the bands immediately adjacent to the gap.¹¹ GeS, with its larger band gap, might produce a band alignment such that the valence bands of SnS and GeS would have a small offset and the conduction band of GeS would lie higher in energy than that of SnS, allowing it to indeed play the role of the electron-blocking layer in a SnS solar device.

The aim of this paper is to employ *ab initio* methods in order to evaluate the above possibility. To this end, we construct explicit interface models of SnS and GeS along the three principal directions of their orthorhombic unit cells in order to evaluate the band offsets. Since the value of the conduction band offset in the interface model is directly related to the value of the band gaps on each side of the interface, we employ

quasiparticle energy corrections within the framework of the *GW* approximation to the electron self-energy. The calculated band gaps obtained in this way not only allow us to evaluate the band offsets, but help shed light on these important intrinsic properties of the materials themselves, which at present are not well established. The paper is organized as follows: In Sec. II the computational details employed in the present calculations are discussed. In Sec. III the results are presented, beginning with the density-functional-theory (DFT) results in Sec. III A and followed by the results incorporating the quasiparticle corrections in Sec. III B. The construction of the interface models and the evaluation of the resulting band offsets are described in Sec. III C. We then end with some concluding remarks in Sec. IV.

II. METHODS

The majority of the calculations performed in this paper are done within the framework of the local density approximation (LDA) to density functional theory (DFT). The calculations of the quasiparticle self-energy corrections, while extending beyond DFT, use DFT wave functions and energies as a mean-field starting point. The DFT calculations are performed using the plane-wave pseudopotential method^{12,13} as implemented within the QUANTUM-ESPRESSO package.¹⁴ Norm-conserving pseudopotentials for Sn, Ge, and S are generated with the APE pseudopotential generator.¹⁵ The states treated as valence in Ge, Sn, and S were the $4s^2 4p^2$ states, the $5s^2 5p^2$ states, and the $3s^2 3p^4$ states, respectively. For calculations on bulk SnS and GeS, the wave functions are expanded in plane waves with a kinetic energy cutoff of 50 Ry. At this cutoff the total energy is converged to within 0.23 and 0.18 mRy/atom in SnS and GeS, respectively. A higher plane-wave cutoff of 80 Ry was used during structural relaxations in order to have a highly converged stress tensor, which typically converges more slowly with respect to the energy cutoff than the total energy. For the interface calculations a lower cutoff of 45 Ry was used in order to obtain results on the large interface models at a lower computational cost. The total energy of the interface calculations was still converged to within 0.5 mRy/atom at this lower energy cutoff. As we will describe, relaxations of

the cell shape were not needed in performing the calculations on the interface models and thus a higher energy cutoff to converge the stress tensor would not have been useful in this case. The sampling of the Brillouin zone (BZ) used for the bulk materials was a mesh of size $5 \times 6 \times 2$, which converges the total energy in SnS and GeS to within less than 0.2 mRy/atom. In order to obtain higher quality stress tensors and pressures, a finer grid of size $10 \times 12 \times 4$ was used in the relaxations, which produces negligible differences in pressure from the infinite sampling limit. Brillouin zone samplings required in the calculation of the quasiparticle energies and the study of the interfaces will be presented along with the discussion of the corresponding results.

III. RESULTS

A. LDA calculations

SnS and GeS have a layered crystal structure with space group D_{2h}^{16} containing eight atoms in the primitive unit cell.^{16,17} The experimental parameters used for SnS in this paper are from Ref. 18: $a = 4.334 \text{ \AA}$, $b = 3.987 \text{ \AA}$, and $c = 11.20 \text{ \AA}$ with internal parameters of $u(\text{Sn}) = 0.1198$, $u(\text{S}) = 0.4793$, $w(\text{Sn}) = 0.1194$, and $w(\text{S}) = -0.1492$. The experimental parameters used for GeS are from Ref. 17: $a = 4.30 \text{ \AA}$, $b = 3.64 \text{ \AA}$, and $c = 10.47 \text{ \AA}$ with internal parameters $u(\text{Ge}) = 0.127$, $u(\text{S}) = 0.499$, $w(\text{Ge}) = 0.122$, and $w(\text{S}) = -0.151$. A representation of the structure common to both SnS and GeS is shown in Fig. 1.

The LDA band structure of SnS at the experimental structural parameters is shown in Fig. 2(a). The band gap of 0.72 eV is indirect with the valence band maximum (VBM) occurring $\sim 88\%$ of the way to X along the Γ -X line. The conduction band minimum (CBM) lies along the line connecting Γ and Y, approximately 63% of the way to Y. From the band structure it can be seen that there are nearby competing extrema in both the valence and conduction

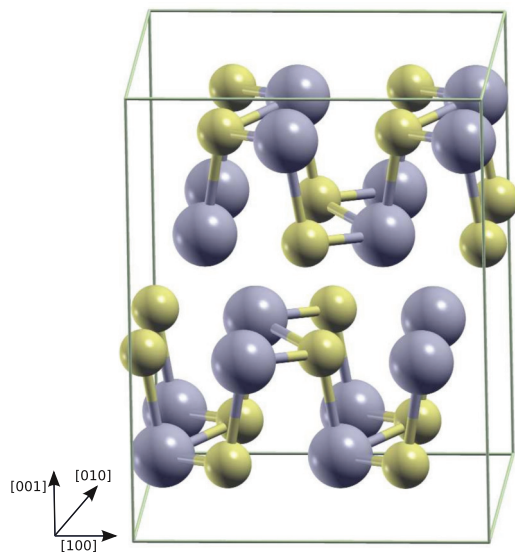


FIG. 1. (Color online) The layered structure of SnS and GeS. Sn/Ge atoms are displayed in gray while S is in yellow. We show a $2 \times 2 \times 1$ multiple of the eight-atom unit cell for better visualization.

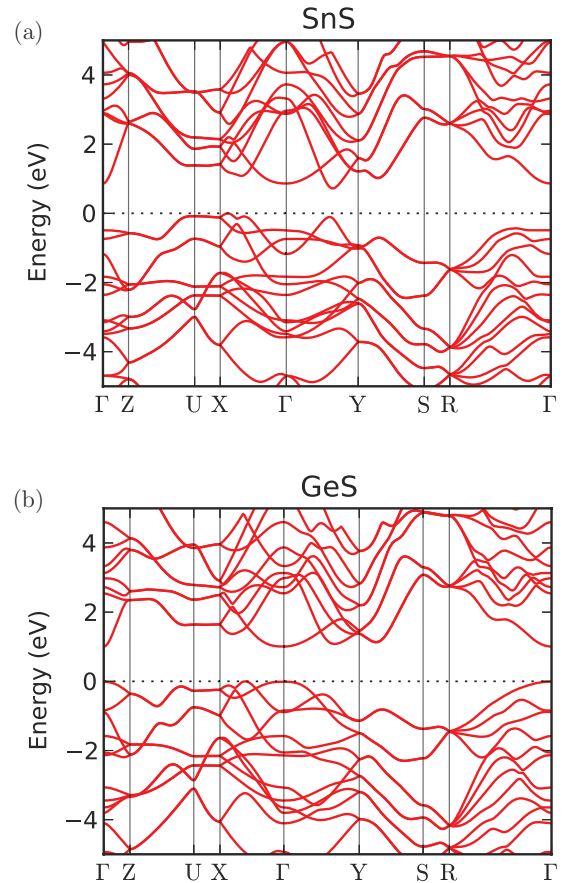


FIG. 2. (Color online) LDA band structure of (a) SnS and (b) GeS, at the experimental structure. The zero of energy is set to the valence band maximum in each case.

bands.^{11,19} Because these competing band extrema are close in energy, different band gaps can be obtained depending on the choice of exchange-correlation functional and whether or not the band structure is computed at the experimental or the theoretical values for the lattice constants. For this reason we do not make a comparison of these gaps to other published results.

The band structure of GeS at the LDA level is depicted in Fig. 2(b). The LDA band gap of 1.00 eV is indirect between the VBM located $\sim 60\%$ along the Γ -X line and the CBM at Γ . As in the case for SnS, competing band edges can be seen in this band structure as well and different choices of exchange-correlation functional or relaxation of the lattice can alter the location of the band extrema. Indeed, if we relax the structure with the LDA functional and then compute the band structure, we find that the gap is direct at Γ with a value of 0.78 eV. A summary of the experimental and theoretical structural parameters used in this paper is presented in Table I alongside the band gaps computed within LDA for each structure.

B. GW calculations

Both SnS and GeS are of interest in potential device applications because of the intermediate-sized band gaps, so an accurate determination of the gap is important. There is some variation in the experimental values for these band gaps,

TABLE I. Structural parameters of SnS and GeS used in this paper. Experimental parameters are taken from Refs. 18 and 17 for SnS and GeS, respectively. Relaxed structures are obtained from first-principles relaxation using the LDA functional. In the final column we present the fundamental gap at the LDA level for each structure.

	a (Å)	b (Å)	c (Å)	u (Sn/Ge)	w (Sn/Ge)	u (S)	w (S)	E_g^0 (eV) (LDA)
SnS								
Expt.	4.334	3.987	11.20	0.1198	0.1194	0.4793	-0.1492	0.72
Relaxed	4.27	3.88	10.91	0.117	0.118	0.478	-0.146	0.40
GeS								
Expt.	4.30	3.64	10.47	0.127	0.122	0.499	-0.151	1.00
Relaxed	4.29	3.51	10.22	0.127	0.122	0.512	-0.152	0.78

although some differences are due to temperature effects. When band gaps are extrapolated to zero temperature using published values of the temperature coefficient of the gap, the experimental values fall within a reasonably narrow range. However, existing *GW* calculations on SnS and GeS (Refs. 9,20) agree better with the room-temperature values of the experimentally reported band gaps and show larger deviations for the zero-temperature values to which they should be compared. With experimentally measured temperature coefficients of -0.437 meV/K (Ref. 16) and -0.52 meV/K (Ref. 21) for SnS and GeS, respectively, room-temperature band gaps can be expected to differ from zero-temperature gaps by ~ 0.15 eV. Since band alignments depend on the band gap values on both sides of the interface, we performed carefully converged calculations of the band gap within the *GW* approximation to the self-energy in order to resolve the discrepancy in the experimental and theoretical values.

Our *GW* calculations are done using the BERKELEYGW package²² which interfaces with QUANTUM ESPRESSO. Calculations are carried out within the “single-shot” *GW* approach, also referred to as G_0W_0 .^{23,24} The dynamical screening in the self-energy is taken into account by a generalized plasmon-pole model which extends the static dielectric function calculated from first principles to finite frequencies.^{24,25}

In the calculation of the *GW* correction to the band gap, a number of computational parameters are involved which affect the precision of the final value. In the expression for the self-energy, these include summations over reciprocal lattice vectors, summations over unoccupied states, and Brillouin zone summations.^{22,24} The calculation of the screened Coulomb interaction W also has a summation over unoccupied bands that must be carefully considered.^{22,24} As discussed in Ref. 26, these parameters are not all independent of one another, and thus some care must be taken in order to estimate uncertainties in the precision of the calculation. In the Supplemental Material we describe the procedure used to estimate the precision of the *GW* results reported in this paper, which is on the level of ~ 50 meV or better.²⁷

Our quasiparticle calculations on SnS at the experimental lattice constants produce an indirect band gap of 1.26 eV. This value is obtained by calculating the quasiparticle energy corrections for the points determined to be the band extrema in the LDA calculation. This is well justified as long as the quasiparticle corrections themselves do not vary strongly between different wave vectors. Vidal *et al.*⁹ found that the quasiparticle shifts were relatively uniform and did not change

the underlying locations of the band extrema from those in DFT. From our calculations we find that this is likely the case: Both the valence band and conduction band quasiparticle energy corrections are clustered around their respective full BZ average with a half-width of approximately 50 meV.²⁷ Since 50 meV is our estimated precision in the calculations themselves, it is not even reliable to analyze these results further for possible changes of the band extrema.

We will now compare our calculated band gap of 1.26 eV to published results. While the quasiparticle energies calculated here can only rigorously be compared to photoemission-related experiments where an electron is either added or removed from the solid, we are unaware of any experimental determinations of the band gap using such methods. Therefore we compare our calculated values with the available experimental data, primarily obtained from optical absorption measurements. It should be noted that these measurements may include electron-hole interaction effects which are not considered in this paper. Similar limitations in comparisons to the experimental data are present for GeS. Also, as many of the experimental measurements are taken at room temperature, we adjust all values by the temperature coefficient of the band gap in order to obtain values which better approximate the situation at zero temperature. In cases where no temperature dependence of the gap has been measured in the experiment, we use the temperature coefficient of -0.437 meV/K from Ref. 16 in order to extrapolate to zero temperature. These results are summarized in Table II. As can be seen from the table, the range of experimental values for SnS is relatively narrow, with most values falling within roughly 0.1 eV of 1.25 eV. Our calculated value of 1.26 eV compares very favorably with these numbers. Other quasiparticle corrections using the *GW* method have obtained a smaller value of 1.07 eV,^{9,20} which is in good agreement with some of the earliest experimental band gap estimates at finite temperatures, but compares less favorably when the band gap is extrapolated to zero temperature where the theoretical results are valid. The cause of the 0.21 eV discrepancy between the present results and the prior theory results is unclear, but different *GW* methodologies and/or differing levels of convergence could easily account for such differences. Additionally, the *GW* calculations of Ref. 20 was performed for a SnS structure that was theoretically determined and not taken from experiment. This choice will also lead to further differences in the results (see Table I).

For GeS, we obtain a *GW* correction of 0.74 eV to the LDA band gap value of 1.00 eV, giving a quasiparticle gap

TABLE II. Comparison of the calculated gap for SnS presented in this paper with other published values, both experimental and theoretical. Experimental values published at finite temperatures are extrapolated to zero temperature using the temperature coefficient from Ref. 16 (-0.437 meV/K) with the exception of the results of Ref. 28 (-0.36 meV/K) and Ref. 29 (-0.121 meV/K). All experimental results are based on optical absorption measurements.

	T (K)	$E_g^{(T)}$ (eV)	E_g^0 (eV)
Theory			
Present work			1.26
Ref. 9 (<i>GW</i>)			1.07
Ref. 20 (<i>GW</i>)			1.07
Experiment			
Ref. 30	298	1.07	1.20
Ref. 16	100	1.18	1.22
Ref. 31	473	1.16	1.37
Ref. 5	298	1.18	1.31
Ref. 28	295	1.05	1.16
Ref. 29	4	1.5	1.5

of 1.74 eV. Similar to the case for SnS, the values of the quasiparticle corrections were calculated at the band extrema found in the LDA calculation to determine the final band gap. In GeS the valence and conduction band quasiparticle shifts are again nearly constant throughout the Brillouin zone, deviating by only a small amount (~ 50 meV) from the Brillouin zone average.²⁷

In Table III we summarize experimental information on the GeS band gap, which indicates that the band gap is near 1.75 eV, close to the result calculated using *GW* in this paper. The *GW* calculation presented in Ref. 20 is an available theoretical value of the band gap with which we can compare our result. This calculation agrees much better with some of the room-temperature experimental values, but shows a larger discrepancy with the value extrapolated to

TABLE III. Comparison of the calculated gap for GeS presented in this paper with other values, both experimental and theoretical, found in the literature. Experimental values of the optical gaps taken at finite temperatures are extrapolated to zero temperature using the temperature coefficient found in Ref. 21 (-0.52 meV/K). All experimental results are based on optical absorption, except those of Ref. 32, which are from photoconductivity. The photoconductivity results were extrapolated using the temperature coefficient in Ref. 32 (-0.43 meV/K).

	T (K)	$E_g^{(T)}$ (eV)	E_g^0 (eV)
Theory			
Present work			1.74
Ref. 20 (<i>GW</i>)			1.53
Experiment			
Ref. 33	300	1.65	1.81
Ref. 34	4.2	1.74	1.75
Ref. 21	298	1.54	1.70
Ref. 35	298	1.8	1.96
Ref. 36	298	1.58	1.74
Ref. 32	298	1.61	1.74

zero temperature. The calculation in Ref. 20 was also done at the theoretically determined structure, which will cause additional discrepancies in the comparison of our results beyond those from differing methodologies or levels of convergence.

C. Interface band offsets

We now turn to the evaluation of the band offsets between SnS and GeS. With the motivation that GeS could serve as a functional layer in a SnS-based photovoltaic device, the small lattice mismatch between the two isostructural materials is relieved in the calculation by straining GeS to the lattice constant of SnS (that is, treating SnS as the substrate). We investigate three different interface orientations, namely, the [100], [010], and [001] directions as defined in Fig. 1. Structural models of the [100], [010], and [001] interfaces are shown in Fig. 3. To construct each particular interface model, the other two directions of the GeS unit cell are strained to the SnS substrate values. This strained GeS unit cell is allowed to fully relax, including cell relaxation in the direction normal to the interface, using the higher energy cutoff of 80 Ry, as specified in Sec. II. Following this relaxation, the interface model is produced between SnS and GeS by expanding the primitive cells in the direction normal to the interface forming a superlattice of SnS/GeS. The final structure is then allowed to relax to accommodate changes caused by the formation of the interface between the two materials. The number of layers on either side of the interface is increased until a negligible change in the computed quantities is achieved. The number of layers used for each interface orientation is included in Table IV.

The band offsets between two materials cannot be computed from the two bulk calculations alone, which lack a common reference energy with which to align the band edges to each other. The presence of the interface allows the computation of the discontinuity in the electrostatic potential caused by the interface, ΔV . Far from the interface the electrostatic potential will assume its value in the bulk. In this way the valence band edges in the bulk crystals, referred to the average electrostatic potential in the bulk cells, can be related to each other by the offset ΔV . Further details of this methodology can be found in Ref. 37. In Fig. 3 we show the planar-averaged electrostatic potential for the [100], the [010], and the [001] interface between SnS and GeS. Averaging over the bulklike region far from the interface results in the values \bar{V}_{SnS} and \bar{V}_{GeS} which are related to ΔV as $\Delta V = \bar{V}_{\text{SnS}} - \bar{V}_{\text{GeS}}$.

TABLE IV. Summary of results on the SnS/GeS interface for different interface orientations. N_{layer} is the number of layers of each material on either side of the interface. ΔV is the discontinuity in the electrostatic potential, VBO is the valence band offset, and CBO is the conduction band offset. The sign of the offset is given as $E_{\text{SnS}} - E_{\text{GeS}}$.

	N_{layer}	ΔV (eV)	VBO (eV)	CBO (eV)
[100]	8	0.47	0.45	-0.20
[010]	12	0.91	0.47	0.19
[001]	6	0.63	0.41	0.05

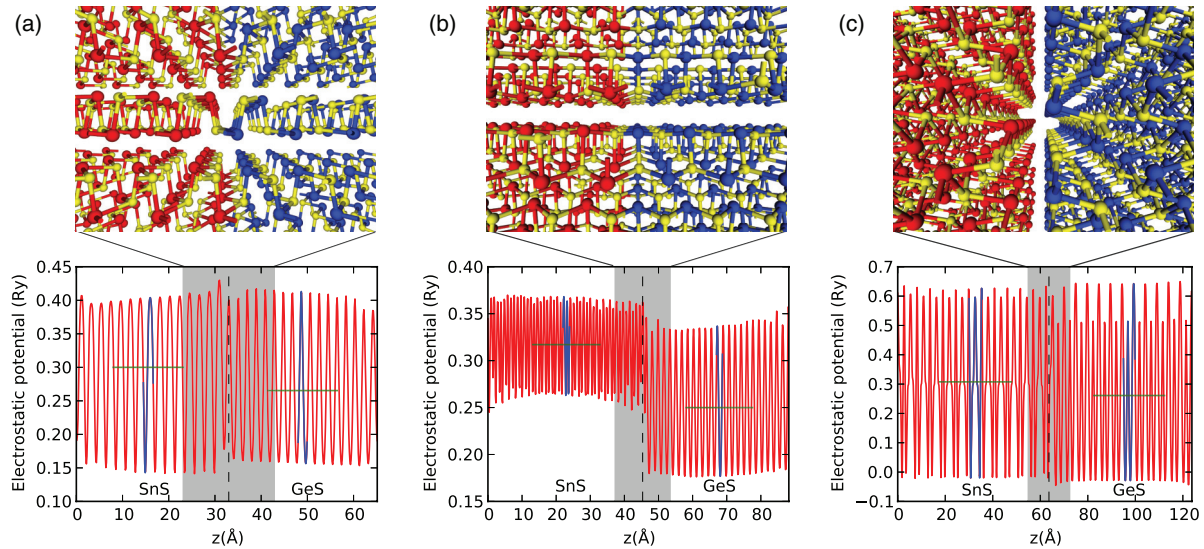


FIG. 3. (Color online) The structural models (top) and planar-averaged electrostatic potentials (bottom) of the (a) [100], (b) [010], and (c) [001] SnS-GeS interfaces. The blue overlay indicates the bulklike region of the electrostatic potential which is averaged over a period to obtain the averages \bar{V}_{SnS} and \bar{V}_{GeS} , shown in green. The discontinuity in the electrostatic potential due to the interface is $\Delta V = \bar{V}_{\text{SnS}} - \bar{V}_{\text{GeS}}$.

The computed results for the band offsets between SnS and GeS are summarized in Table IV and indicated schematically in Fig. 4. The valence band offset (VBO) between the materials can be obtained from the calculations described above at the DFT level. However, this assumes that the valence band edges on either side of the interface shift equally under the influence of the quasiparticle corrections in relation to their respective electrostatic potential averages. Therefore we have carried out additional *GW* calculations on the theoretically relaxed structures, including the GeS cells which have been strained to the SnS substrate parameters. We find that the shifts in the VBM for the strained GeS cells are between 0.2 and 0.3 eV larger than the shift in the VBM for SnS at the theoretically relaxed structure, and this contributes to commensurate increases in the valence band offsets relative to what would have been obtained using only the DFT values. The conduction band offset can be obtained in a couple of different ways. One option is to use the band gap values from the *GW* calculations on either side of the interface to establish a conduction band offset. Another option is to use the band gap values determined on the experimental structures, as shown in Tables II and III. In this case the value of the GeS band gap of 1.74 eV is adjusted from its unstrained value because of the strain introduced by the SnS substrate, a change which depends on the orientation. This amount can be determined by the difference in the *GW* band gaps between the GeS unstrained structure and the GeS strained structures, both relaxed theoretically. In this paper we take the latter approach for the reason that the calculated *GW* band gaps on the experimental structures are more likely to represent the experimental band gaps. The two different approaches will produce slightly different results because the difference in quasiparticle band gap between SnS and GeS depends on whether both materials are taken at the experimental structure or the theoretically relaxed structure. This difference, taken as $E_g^{\text{GeS}} - E_g^{\text{SnS}}$, is larger for the theoretically determined structures by almost 0.2 eV.

It is apparent from the results shown that the valence band offset is almost isotropic, varying little between different interface orientations, with the SnS valence band lying higher in energy than that of GeS. Such a situation is not ideal if the layer is to be used as an electron-blocking layer because it presents a barrier to hole transport as well. The conduction band offsets, on the other hand, show a strong variation depending on the interface orientation. For the [100] interface, the GeS conduction band lies higher than that of SnS by 0.20 eV. In contrast, for the [010] and [001] directions, the GeS band actually lies slightly lower in energy than that in the SnS layer by 0.19 and 0.05 eV, respectively, leading to the formation of a type II heterojunction. This anisotropy is caused by the response of the band gap to the different strain applied in forming the heterojunction orientations. For example, the strain required in GeS to match SnS for the [100] interface causes the band gap to increase by 0.17 eV, whereas for the [010] interface the band gap of GeS shows a decrease of 0.21 eV due to the applied strain.

IV. CONCLUSION

In this paper we present an analysis of the electronic structure of SnS and GeS, both at the LDA level and at the *GW* level for the electron self-energy. Our LDA calculations confirm the existence of the competing band extrema that have been discussed in prior works which may be the cause of some of the discrepancy in the literature in regards to the nature of the fundamental gap. Our *GW* calculations on the experimental structures of SnS and GeS result in indirect band gaps of 1.26 and 1.74 eV, respectively, in excellent agreement with the available experimental results that have been extrapolated to zero temperature.

We also investigate the interface physics of SnS/GeS heterojunctions, in order to obtain the band offsets which are one of the fundamental quantities determining the possible role of GeS layers in a SnS-based photovoltaic device. We

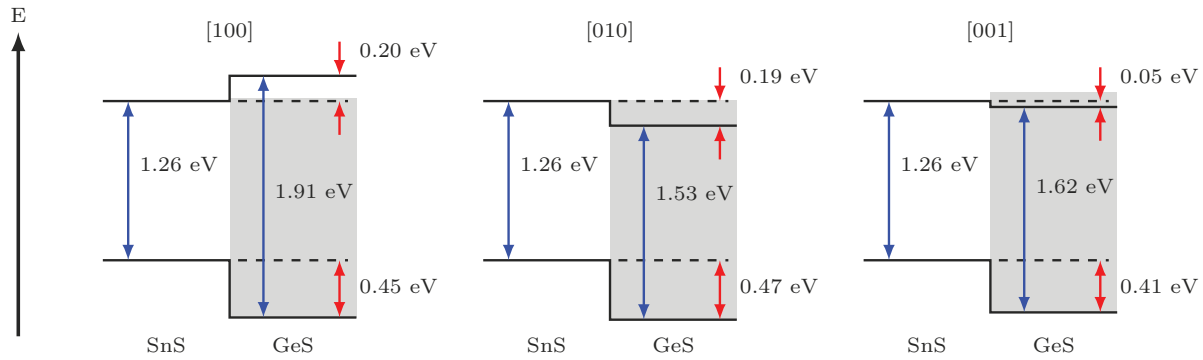


FIG. 4. (Color online) The calculated band offsets of the SnS-GeS interface along the [100], [010], and [001] orientations. The arrows in red denote the band offsets and those in blue denote the band gaps on either side of the interface. The GeS gap varies with the interface orientation because of the strain applied to match the SnS substrate. Its unstrained value of 1.74 eV is shown as the shaded region. See the text for more details.

find that while the valence band offsets are fairly isotropic, the conduction band offsets are markedly anisotropic, ranging from -0.20 to $+0.19$ eV, due to the varying response of the GeS band gap to epitaxial strain imposed on the GeS lattice to fit on the SnS substrate in the different interfacial orientations. The [100] interface appears to be the most promising in terms of using GeS as an electron-blocking layer because it has an energetic barrier of 0.20 eV for electrons in SnS to escape to the GeS layer. However, for all orientations we predict a offset in the valence band of ~ 0.44 eV on average, which would undesirably inhibit the transport of holes. Unless this hole barrier could be reduced by some means such as doping,

GeS may not exhibit band offsets with SnS, which are useful for use as an electron-blocking layer.

ACKNOWLEDGMENTS

We thank Roy G. Gordon and Prasert Sinsersuksakul for helpful and ongoing discussions. Additionally, we thank Chris Van de Walle for useful comments and suggestions. Computational resources were provided by the Extreme Science and Engineering Discovery Environment (XSEDE), supported by NSF Grant No. TG-DMR120073.

¹C. Wadia, A. P. Alivisatos, and D. M. Kammen, *Environ. Sci. Technol.* **43**, 2072 (2009).

²K. T. R. Reddy, N. K. Reddy, and R. W. Miles, *Sol. Energy Mater. Sol. Cells* **90**, 3041 (2006).

³P. Sinsersuksakul, J. Heo, W. Noh, A. S. Hock, and R. G. Gordon, *Adv. Energy Mater.* **1**, 1116 (2011).

⁴R. W. Miles, O. E. Ogah, G. Zoppi, and I. Forbes, *Thin Solid Films* **517**, 4702 (2009).

⁵K. Hartman, J. L. Johnson, M. I. Bertoni, D. Recht, M. J. Aziz, M. A. Scarpulla, and T. Buonassisi, *Thin Solid Films* **519**, 7421 (2011).

⁶G. Yue, Y. Lin, X. Wen, L. Wang, and D. Peng, *J. Mater. Chem.* **22**, 16437 (2012).

⁷P. Sinsersuksakul, K. Hartman, S. B. Kim, J. Heo, L. Sun, H. H. Park, R. Chakraborty, T. Buonassisi, and R. G. Gordon, *Appl. Phys. Lett.* **102**, 053901 (2013).

⁸H. Noguchi, A. Setiyadi, H. Tanamura, T. Nagatomo, and O. Omoto, *Sol. Energy Mater. Sol. Cells* **35**, 325 (1994).

⁹J. Vidal, S. Lany, M. d' Avezac, A. Zunger, A. Zakutayev, J. Francis, and J. Tate, *Appl. Phys. Lett.* **100**, 032104 (2012).

¹⁰R. G. Gordon (private communication).

¹¹G. A. Tritsarlis, B. D. Malone, and E. Kaxiras, *J. Appl. Phys.* **113**, 233507 (2013).

¹²J. Ihm, A. Zunger, and M. L. Cohen, *J. Phys. C: Solid State Phys.* **12**, 4409 (1979).

¹³M. L. Cohen, *Phys. Scr., T* **1**, 5 (1982).

¹⁴P. Giannozzi, S. Baroni, N. Bonini, M. Calandra, R. Car, C. Cavazzoni, D. Ceresoli, G. L. Chiarotti, M. Cococcioni, I. Dabo *et al.*, *J. Phys.: Condens. Matter* **21**, 395502 (2009).

¹⁵M. J. T. Oliveira and F. Nogueira, *Comput. Phys. Commun.* **178**, 524 (2008).

¹⁶A. P. Lambros, D. Geraleas, and N. A. Economou, *J. Phys. Chem. Solids* **35**, 537 (1974).

¹⁷T. Grandke and L. Ley, *Phys. Rev. B* **16**, 832 (1977).

¹⁸H. Wiedemeier and H. G. von Schnering, *Z. Kristallogr.* **148**, 295 (1978).

¹⁹L. Makinistian and E. A. Albanesi, *Phys. Status Solidi B* **246**, 183 (2009).

²⁰L. Makinistian and E. A. Albanesi, *Comput. Mater. Sci.* **50**, 2872 (2011).

²¹A. M. Elkorashy, *J. Phys. C: Solid State Phys.* **21**, 2595 (1988).

²²J. Deslippe, G. Samsonidze, D. A. Strubbe, M. Jain, M. L. Cohen, and S. G. Louie, *Comput. Phys. Commun.* **183**, 1269 (2012).

²³W. G. Aulbur, L. Jönsson, and J. W. Wilkins, in *Solid State Physics*, edited by H. Ehrenreich and F. Spaepen (Academic, New York, 2000), Vol. 54.

²⁴M. S. Hybertsen and S. G. Louie, *Phys. Rev. B* **34**, 5390 (1986).

²⁵M. S. Hybertsen and S. G. Louie, *Phys. Rev. Lett.* **55**, 1418 (1985).

- ²⁶B. D. Malone and M. L. Cohen, *J. Phys.: Condens. Matter* **25**, 105503 (2013).
- ²⁷See Supplemental Material at <http://link.aps.org/supplemental/10.1103/PhysRevB.87.245312> for a description of the procedure used to estimate the precision of the *GW* results reported in this paper.
- ²⁸M. Parenteau and C. Carlone, *Phys. Rev. B* **41**, 5227 (1990).
- ²⁹N. K. Reddy, Y. B. Hahn, M. Devika, H. R. Sumana, and K. R. Gunasekhar, *J. Appl. Phys.* **101**, 093522 (2007).
- ³⁰W. Albers, C. Haas, and F. van der Maesen, *J. Phys. Chem. Solids* **15**, 306 (1960).
- ³¹A. Ortiz, J. C. Alonso, M. Garcia, and J. Toriz, *Semicond. Sci. Technol.* **11**, 243 (1996).
- ³²A. M. Elkorashy, *J. Phys.: Condens. Matter* **2**, 6195 (1990).
- ³³R. Eymard and A. Otto, *Phys. Rev. B* **16**, 1616 (1977).
- ³⁴J. D. Wiley, A. Breitschwerdt, and E. Schönherr, *Solid State Commun.* **17**, 355 (1975).
- ³⁵J. H. Haritonidis and D. S. Kyriakos, *Semicond. Sci. Technol.* **4**, 365 (1989).
- ³⁶D. D. Vaughn II, R. J. Patel, M. A. Hickner, and R. E. Schaak, *J. Am. Chem. Soc.* **132**, 15170 (2010).
- ³⁷C. G. Van de Walle and R. M. Martin, *Phys. Rev. B* **35**, 8154 (1987).